UCRL-16942

University of California
Ernest O. Lawrence Radiation Laboratory

DISLOCATION DAMPING IN ZINC SINGLE CRYSTALS

Berkeley, California

DISCLAIMER

Submitted to Acta Met.

UCRL-16942
Preprint

UNIVERSITY OF CALIFORNIA

Lawrence Radiation Laboratory
Berkeley, California

AEC Contract No. W-7408-eng-48

DISLOCATION DAMPING IN ZINC SINGLE CRYSTALS

W. G. Ferguson, F. E. Hauser and J. E. Dorn

August, 1966

DISLOCATION DAMPING IN ZINC SINGLE CRYSTALS

W. G. Ferguson, F. E. Hauser and J. E. Dorn

Inorganic Materials Research Division, Lawrence Radiation Laboratory, and Department of Mineral Technology, College of Engineering University of California, Berkeley, California

August, 1966

ABSTRACT

Impact shear tests of the Kolsky Thin Wafer type were used to determine the effects of temperature and strain rate on the critical resolved shear stress for basal slip in zinc single crystals. At the high strain rates the flow stress was found to increase linearly with the plastic strain rate and was independent of temperature. The observed behavior could be rationalized in terms of Mason's dislocation damping model where the friction force acting on a dislocation results from phonon viscosity.

I. INTRODUCTION

Earlier investigations[1,2,3] have shown that in many materials over wide strain rate ranges the effect of the testing temperature on the plastic flow stress can be explained by the mechanism of thermal activation of dislocations over short range barriers. These thermally activated mechanisms of deformation can be visualized as follows. Under an applied shear stress the mobile dislocations move rapidly until various segments meet barriers and the dislocations are held up. After a period of time under the random action of thermal vibration a large enough thermal fluctuation will occur which helps the dislocation to overcome an obstacle and move on. At a given shear stress a higher testing temperature will increase the strain rate because the average arrest periods of the dislocations are decreased. This decrease in arrest time is due to the larger amplitude of thermal vibration and thus a shorter required time for the probability of a thermal activation. Similarly, an increase in shear stress supplies a greater amount of strain energy to the dislocation and a correspondingly smaller thermal fluctuation can activate the process thus decreasing the arrest time and increasing the strain rate.

Figure 1 shows this type of behavior in a schematic way. τ_A is the athermal back stress, that is the back stress due to long range obstacles that cannot be penetrated by the dislocations by means of thermal activation. τ_T is due to short range obstacles and can be overcome by the combination of applied stress ($\tau^* + \tau_A$) plus thermal activation. When the applied stress is higher than $\tau_A + \tau_T$ the dislocations

can be pushed past the barriers without assistance from thermal fluctuations. In this high strain rate, high stress region various energy dissipative mechanisms prescribe the dislocation motion. Of course these mechanisms also dissipate energy at lower stresses and strain rates but there they are not the rate controlling process and thus of second order magnitude compared to dislocation barriers.

It was the object of the present investigation to perform some experiments in the very high stress and strain rate region where one can measure various parameters which may help in identifying the energy dissipative mechanisms governing the motion of high speed dislocations. The results are compared with some of the current dislocation damping theories reviewed previously by Mason,[4,5] Lothe[6] and Dorn, Mitchell and Hauser.[7] Unfortunately all proposed theories predict that the dislocation friction stress should vary linearly with dislocation velocity and thus make it difficult to distinguish between them. However, evidence is presented to show that Mason's phonon viscosity model seems to fit the experimental results best.

II. EXPERIMENTAL TECHNIQUES

In some earlier work in the high stress, high strain rate region by Hauser, Simmons and Dorn[1] on polycrystalline aluminum, the Kolsky Thin Wafer technique[8] and compression specimens were used. It was found that because the material was rather strong and the maximum stress was limited by the impact velocity of the testing machine, little data could be obtained in the high stress range where plastic deformation

is governed only by dislocation damping mechanisms. In subsequent work by Mukherjee, Ferguson, Barmore and Dorn[3] single crystals of β-AgMg were tested in shear impact. Although the shear type specimen permitted higher strain rates because of the smaller effective gauge length, the high strength of the AgMg crystals again limited the available data. Nevertheless, in both prior investigations a linear dependence of flow stress on strain rate was found near the highest possible applied stresses.

In the present investigation zinc single crystals oriented for basal shear were chosen because their low strength permitted very high strain rates to be obtained. The specimens were prepared and tested as follows.

(1) A sphere 1 in diameter was grown in a carbon mold from high purity (99.995 wt. pct.) zinc under an argon atmosphere using the Bridgman technique.

(2) The sphere was used as a seed to grow an oriented single crystal bar with a cross section of 1/4 in. by 1/8 in. with the basal plane perpendicular to the axis of the bar and the slip direction parallel to its 1/4 in. side. The orientation of the crystal bars was checked by the Laue back-reflection x-ray technique and only those found to be within ±1 deg of the required orientation were used.

(3) Specimens 3/8 in. long were cut from the bar and double gauge sections, 0.045 in. long were spark machined in them as shown in Fig. 2a. The spark machined specimens were given a chemical polish in a bath of 1:1 HNO_3 and water to insure all surface deformation from the spark cutting was removed.

(4) The specimens were tested in shear on a specially designed dynamic impact machine by employing the Kolsky technique. The equipmental set-up and the method of analysis has been described previously by Hauser[9] and will not be repeated here apart from showing the configuration of the loading bars used to obtain dynamic shear. Fig. 2b.

(5) Tests above room temperature were conducted using a small Kanthal wound resistance furnace to enclose the specimen.

III. RESULTS AND DISCUSSION

The experimental data obtained are plotted in Fig. 3 as shear stress τ at initial plastic flow versus plastic shear strain rate $\dot{\gamma}$. It can be seen that within the experimental scatter the shear stress is proportional to the shear strain rate and the behavior is independent of temperature. The straight line drawn through the experimental points has the following equation,

$$\tau - \tau_B = \alpha\dot{\gamma} \qquad (1)$$

where τ_B = the back stress as defined in Fig. 3, and α = a constant (5.04×10^3 dyne-sec/cm^2) which is independent of temperature.

The behavior described by Eq. (1) can not be controlled by a thermally activated mechanism. For thermally activated mechanisms $\dot{\gamma} = \dot{\gamma}_o e^{-U/kT}$ where U = some activation energy and kT has the usual meaning. In the high strain rate data presented in Fig. 3, $\dot{\gamma}$ is independent of temperature. Also the slow strain rate data from Fahrenhorst and Schmid[10] shows that the applied stress ($\tau_A + \tau_T$) required to produce plastic deformation

at 0°K is less than the extrapolated back stress τ_B in Fig. 3, indicating that the applied stresses in the present investigation were well above the thermally activated region.

The data in Fig. 3 clearly show that the material is deforming in a viscous manner and hence, the dislocation motion must be damped by some energy absorbing mechanism. Damping of the above type has been observed by a number of investigators[4,5,11] doing internal friction studies. These investigators use the Granato-Lücke[12] theory to obtain a damping constant B defined as follows;

$$F = Bv\,\tau b \qquad (2)$$

where F = the force on the dislocation, v = the dislocation velocity, b = Burger's vector and B = the damping constant. B can be related to α in Eq. (1) by using $\dot{\gamma} = \rho b v$ where ρ is the mobile dislocation density. Then

$$B = \alpha \rho b^2 \qquad (3)$$

Taking $b = 2.67 \times 10^{-8}$ cm for zinc, α from the data = 5×10^3 dynes-sec/cm^2 and assuming $\rho \approx 10^8$ cm^{-2}, then $B = 3.5 \times 10^{-4}$ dyne-sec/cm^2. For comparison, experimental values of B determined by internal friction measurements and direct dislocation velocity measurements, using etch pit techniques,[13,14] are shown in Table 1.

In the high stress region the dislocations are traversing the crystal lattice with little hinderance from lattice imperfections and the dislocation velocity is primarily limited by interactions with electrical and thermal waves. As the electrical interaction is only important

at cryogenic temperatures[5] it will not be discussed here. For thermal waves, at least three mechanisms have been proposed describing the interaction of phonons with dislocations. The first of these, due to Eshelby[20] considers the energy loss associated with the thermoelastic effect as the dislocation moves through the crystal. Since screw dislocations produce only shear stresses in the crystal, the thermoelastic effect which is due to the difference of effective temperature in an extended and compressed lattice does not produce a drag for screw dislocations. Even for edge dislocations this source of phonon damping is much smaller than the other two that will be considered.[16]

The second source of dislocation damping considered is the scattering of thermal phonons by moving dislocations, first derived by Leibfried.[21] The damping constant B for this source of damping takes the form

$$B = \frac{aE_o}{10V_s} \qquad (4)$$

where a = lattice parameter, E_o = thermal energy density, and V_s = shear wave velocity. Taking a = 2.66 x 10^{-8} cm, V_s = 2.41 x 10^5 cm/sec and calculating E_o by numerically integrating the specific heat at constant volume C_v with respect to the temperature T, the magnitude of B for phonon scattering by dislocations in Zn can be obtained as a function of temperature. The results are tabulated in Table 2 and plotted in Fig. 4.

The third source of damping is related to phonon viscosity. This mechanism, first derived by Mason[16,22] regards the lattice vibration as a viscous phonon, gas. When a dislocation moves through this gas,

the gas is stirred up, energy is dissipated and a frictional stress on the dislocation results. The damping constant B for this source of damping takes the form

$$B = \frac{b^2\eta}{8\pi a_o^2} \text{ for screw dislocations} \tag{5}$$

$$B_v = \frac{3}{4}\left\{\frac{b^2\eta}{8\pi(1-\nu)^2 a_o^2}\right\} \text{ for edge dislocations} \tag{6}$$

where b = Burgers vector, a_o = effective core radius of the dislocation, η = viscosity of the phonon gas, and ν = Poisson's ratio. Taking $b = 2.67 \times 10^{-8}$ cm for zinc and using a value of $\frac{3}{4}$ b for a_o as was done by Suzuki, Ikushima and Aoki[11] and Mason,[22] Eq. (5) reduces to

$$B = 0.071\eta \tag{7}$$

η can be shown from gas kinetic theory to be

$$\eta = \frac{D.E_o.K_p}{C_v.\bar{V}^2} \tag{8}$$

where E_o = thermal energy density, K_p = lattice thermal conductivity, $\bar{V}$ = Debye average velocity, C_v = specific heat per unit volume, and D = a nonlinearity constant.

The ratio of the thermal conductivity due to electrons K_e to that due to phonons K_p can be written as[23]

$$\frac{K_e}{K_p} = \frac{C_e}{C_p} \cdot \frac{\bar{U}_e}{\bar{V}} \cdot \frac{\Lambda_e}{\Lambda_p} = \frac{C_e \bar{U}_e^2 \tau_{ep}}{C_v \bar{V}^2 \tau_{pe}} \tag{9}$$

where C_e = the electronic specific heat = $6.04 \times 10^{2} T$ erg/cm -deg, $\bar{U}_e$ = the Fermi velocity of the electrons which for zinc is = 1.35×10^{8}cm/sec and $\frac{\tau_{ep}}{\tau_{pe}}$ = the ratio of the electron-phonon relaxation time to the phonon-electron relaxation time which for metals of good purity is about = 10^{-2}.[23]

Hence from Eqs. (8) and (9)

$$\eta = \frac{D\, E_o\, K_e}{10.9\, T}\, 10^{-16} \text{ dyne-sec/cm}^2 \qquad (10)$$

Taking D = 4 as determined in Appendix 1, E_o as determined above and letting the total thermal conductivity K_T for zinc equal K_e (K_p very small), the magnitude of B for damping by phonon viscosity can be obtained as a function of temperature using Eqs. (7) and (10). The calculations are shown in Table 3 and the results plotted in Fig. 4.

It can be seen from Fig. 4 that the phonon viscosity model predicts a damping constant B which is greater than that predicted by the phonon scattering model and which is also independent of temperature above about 200°K. Although no direct experimental value was obtained for B because of the difficulty of measuring the mobile dislocation density, it can be strongly infered from the data using Eq. (3) that the predominant drag on the dislocations is caused by phonon viscosity. By using the damping constant from the viscosity model and Eq. (3), a mobile dislocation density of $1.7.10^{8}\text{cm}^{-2}$ is obtained which is not unreasonable.

From Eq. (2) it follows that for a shear stress of 3000 psi, taking $B = 4.7 \times 10^{-4}$, the dislocation velocity is about 10^{4} cm/sec,

again a reasonable value. It is interesting to note, that in order for the dislocations to move at the shear wave velocity 2.41 x 10^5cm/sec, the material would have to support a shear stress of about 127,000 psi and be strained at a rate of 2.5 x 10^7 sec^{-1} which cannot be achieved using the Kolsky Thin Wafer technique.

IV. CONCLUSIONS

(1) If zinc is deformed in basal shear at a shear stress higher than the thermally activated stress range it behaves in a viscous manner. In that range the shear stress is proportional to the shear strain rate.

(2) At stresses higher than the thermally activated stress range, the stress-strain rate behavior is independent of temperature for the temperature range investigated, 300°K to 653°K.

(3) Mason's phonon viscosity model for dislocation damping seems to explain the temperature independence of the experimental data whereas the Leibfried phonon scattering model does not.

(4) If one uses the Mason phonon viscosity model and the experimental data in calculating the damping constant, a mobile dislocation density of 1.7 x 10^8 cm^{-2} is predicted for Zn. This reasonable value lends support to the assumed model.

ACKNOWLEDGMENTS

This research was conducted as part of the activities of the Inorganic Materials Research Division of the Lawrence Radiation Laboratory of the University of California. The authors wish to express their appreciation to the United States Atomic Energy Commission for its support of this work.

APPENDIX 1

Estimation of Nonlinearity Constant D

The nonlinearity constant D can be calculated from the third order elastic moduli[4] but as these have not been determined for zinc, a method suggested by Mason[5] was used to obtain an estimate of D. Mason pointed out that it should be possible to separate thermal losses from dislocation losses by measuring the attenuation of longitudinal waves propagated along the c axis of hexagonal crystals. With this mode of propagation dislocations should not be activated. Using the data of Lücke,[24] which is replotted in Fig. 5 and assuming the total attenuation due to thermoelastic and Akheiser[25] losses, a value of D can be obtained from the formulation of the latter type of loss. Lücke has calculated the thermoelastic loss at 100 MC to be 1.72 db/cm, the total loss at this frequency to be 2.02 db/cm and hence the loss due to the Akheiser effect is 0.30 db/cm. The Akheiser loss is similar in principle to a viscosity effect and takes the following formulation for longitudinal waves.[4,5]

$$A = \frac{w^2 \eta}{\rho_m v_e^2} \tag{11}$$

where $w = 2\pi$ times frequency, η = viscosity as defined by Eq. (8), ρ_m = density of material and v_e = longitudinal wave velocity. Taking a frequency at 100 MC, $\rho_m = 7.1$ gm/cc, $v_e = 2.97 \times 10^5$ cm/sec and η as calculated above, then D for longitudinal waves is 8. Mason[5] finds D for shear waves in cadmium to be about half that for longitudinal waves; hence D for shear waves in zinc was taken to be 4.

Table 1. Damping constant B at room temperature.

Material	LiF	NaCl	KCl	Quartz	Cu	Cu-0.13% Mn
Dislocation Velocity Measurements	7×10^{-4}(13)	2×10^{-4}(14)				
Internal Friction Measurements	1.3×10^{-3}(11) 3.4×10^{-4}(19)	2×10^{-3}(15)	3.5×10^{-4}(11)	6×10^{-4}(16)	7.9×10^{-5}(11) 6.0×10^{-5}(16) 8.0×10^{-4}(17) 6.5×10^{-4}(18)	4.5×10^{-4}(11)

Table 2. Calculated values of B for phonon scattering as a function of temperature.

Temperature °K	100	200	300	400	500	600	675
$E_0 \times 10^{-8}$ erg/cm^3	10.8	33.8	58.7	86.1	113.6	142.1	163
$B \times 10^{+5}$ dyne-sec/cm^2	1.2	3.8	6.5	9.5	13	16	18

Table 3. Calculated values of B for phonon viscosity as a function of temperature.

Temperature °K	100	200	300	400	500	600	675
$E_o \times 10^{-8}$ erg/cm^3	10.8	33.8	58.7	86.1	113.6	142.1	163
$K_e \times 10^{-7}$ $\frac{\text{erg}}{\text{sec-cm-deg}}$	1.17	1.15	1.11	1.07	1.03	0.99	0.97
$\eta \times 10^{+3}$ $\frac{\text{dyne-sec}}{\text{cm}^2}$	4.62	7.14	7.96	8.44	8.60	8.60	8.56
B x 10^{-4} $\frac{\text{dyne-sec}}{\text{cm}^2}$	3.3	5.1	5.7	6.0	6.1	6.1	6.1

FIGURE CAPTIONS

Figure 1. Schematic representation of the stress-temperature relationship for thermally activated deformation.

Figure 2a. Specimen geometry.

Figure 2b. Shear bars used for dynamic testing.

Figure 3. Shear stress versus shear strain rate for basal shear in zinc single crystals.

Figure 4. Theoretical damping constants for phonon scattering and phonon viscosity versus temperature.

Figure 5. Attenuation for the propagation of a longitudinal wave along the c-axis of a zinc single crystal.[24]

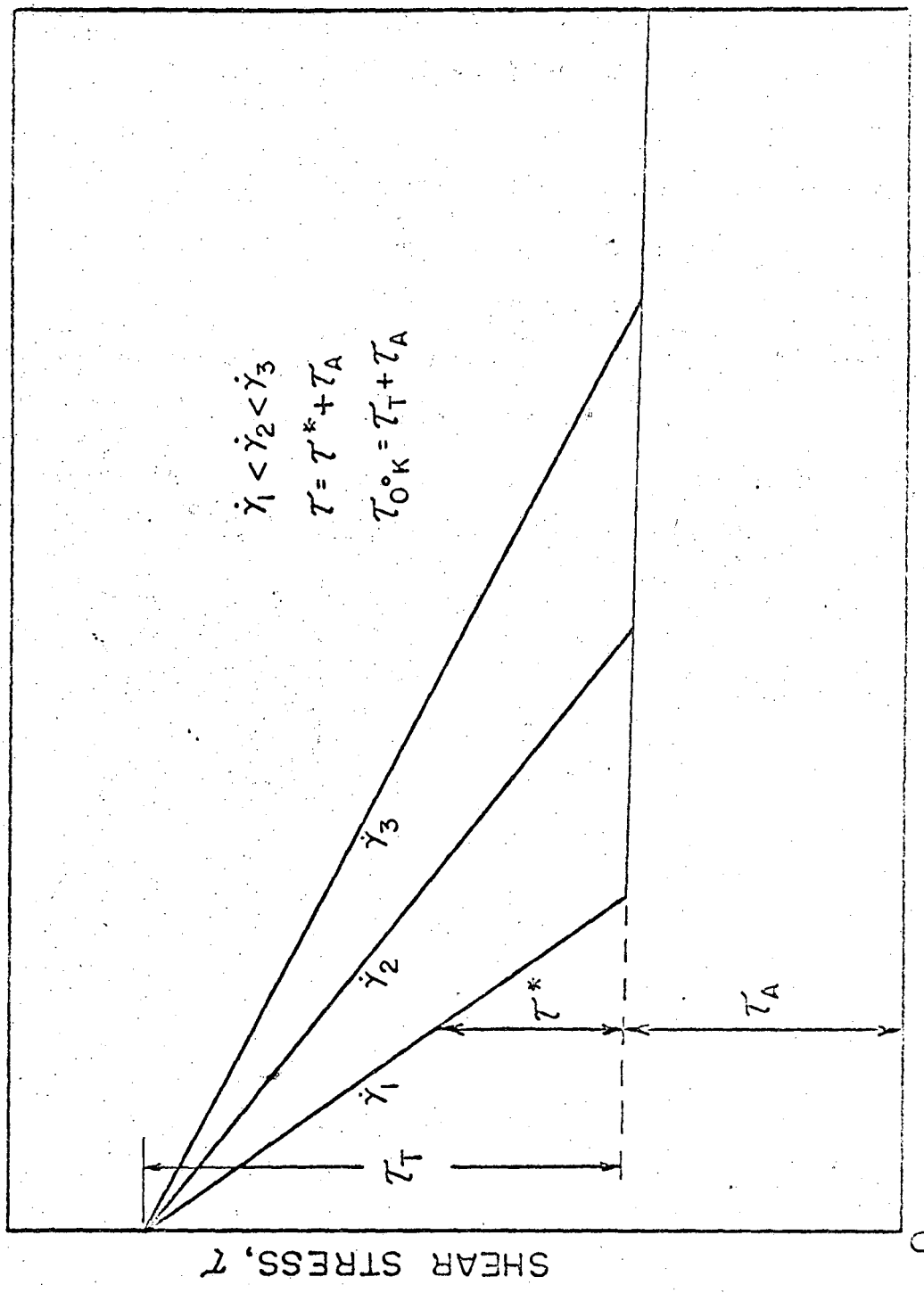

FIG. 1 SCHEMATIC REPRESENTATION OF THE STRESS-TEMPERATURE RELATIONSHIP FOR THERMALLY ACTIVATED DEFORMATION.

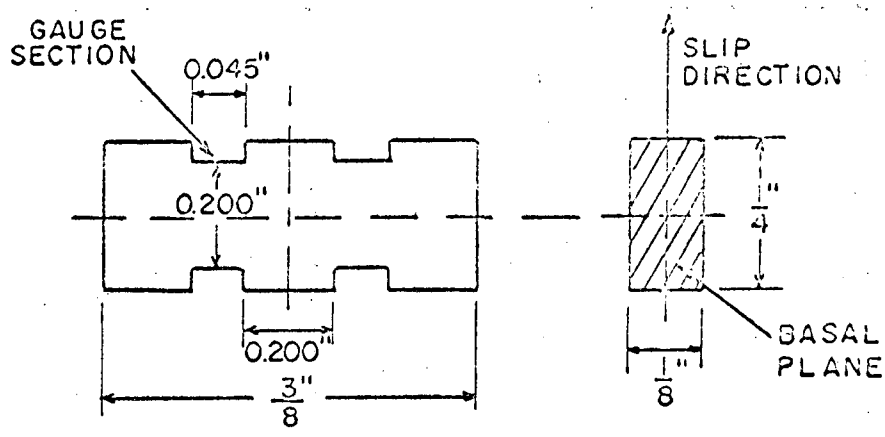

FIG. 2a. SPECIMEN GEOMETRY.

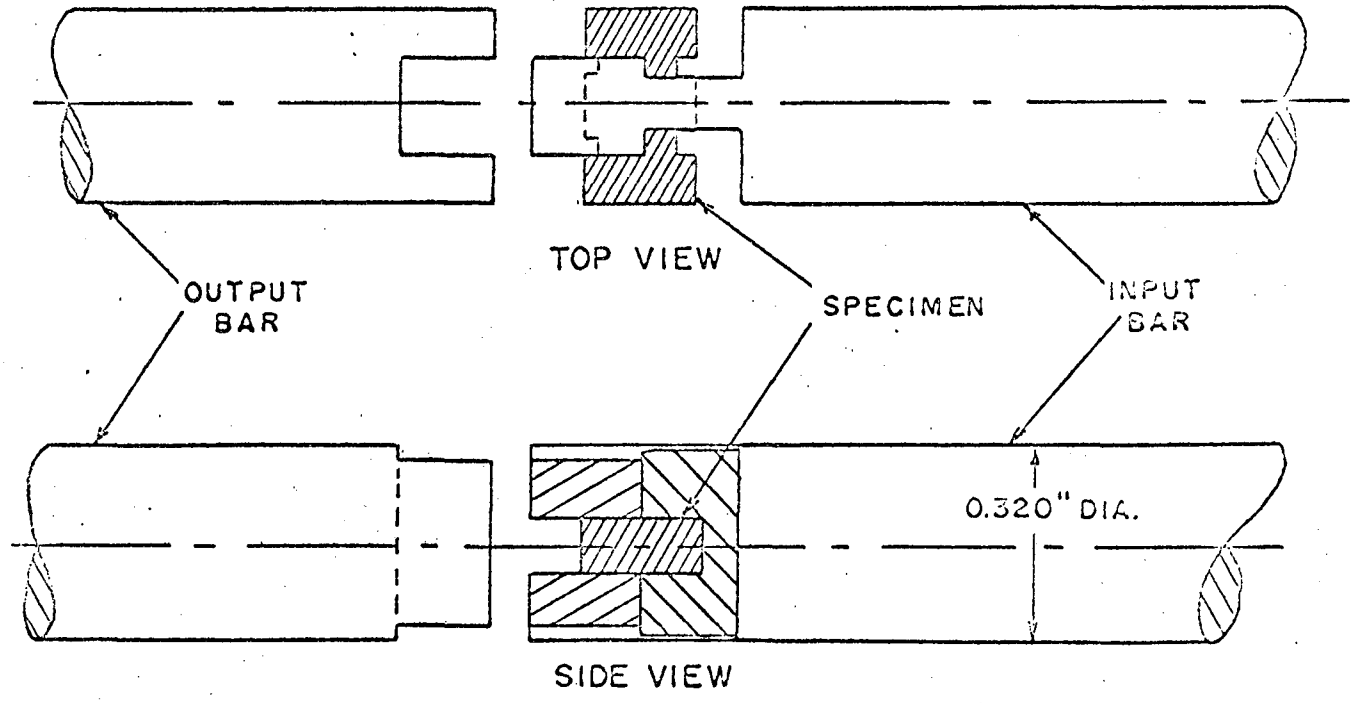

FIG. 2b. SHEAR BARS USED FOR DYNAMIC TESTING.

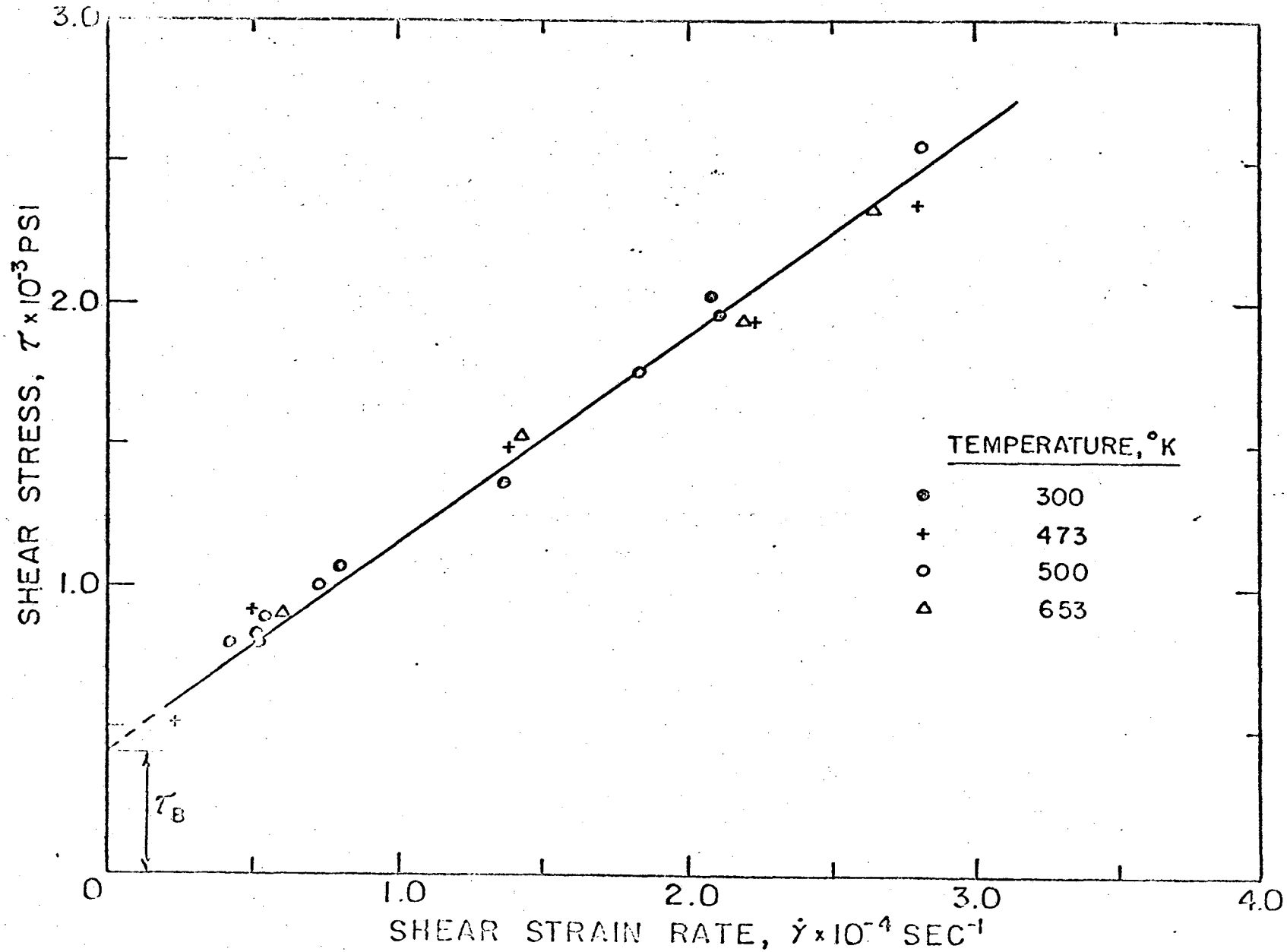

FIG. 3 SHEAR STRESS VERSUS SHEAR STRAIN-RATE FOR BASAL SHEAR IN ZINC SINGLE CRYSTALS.

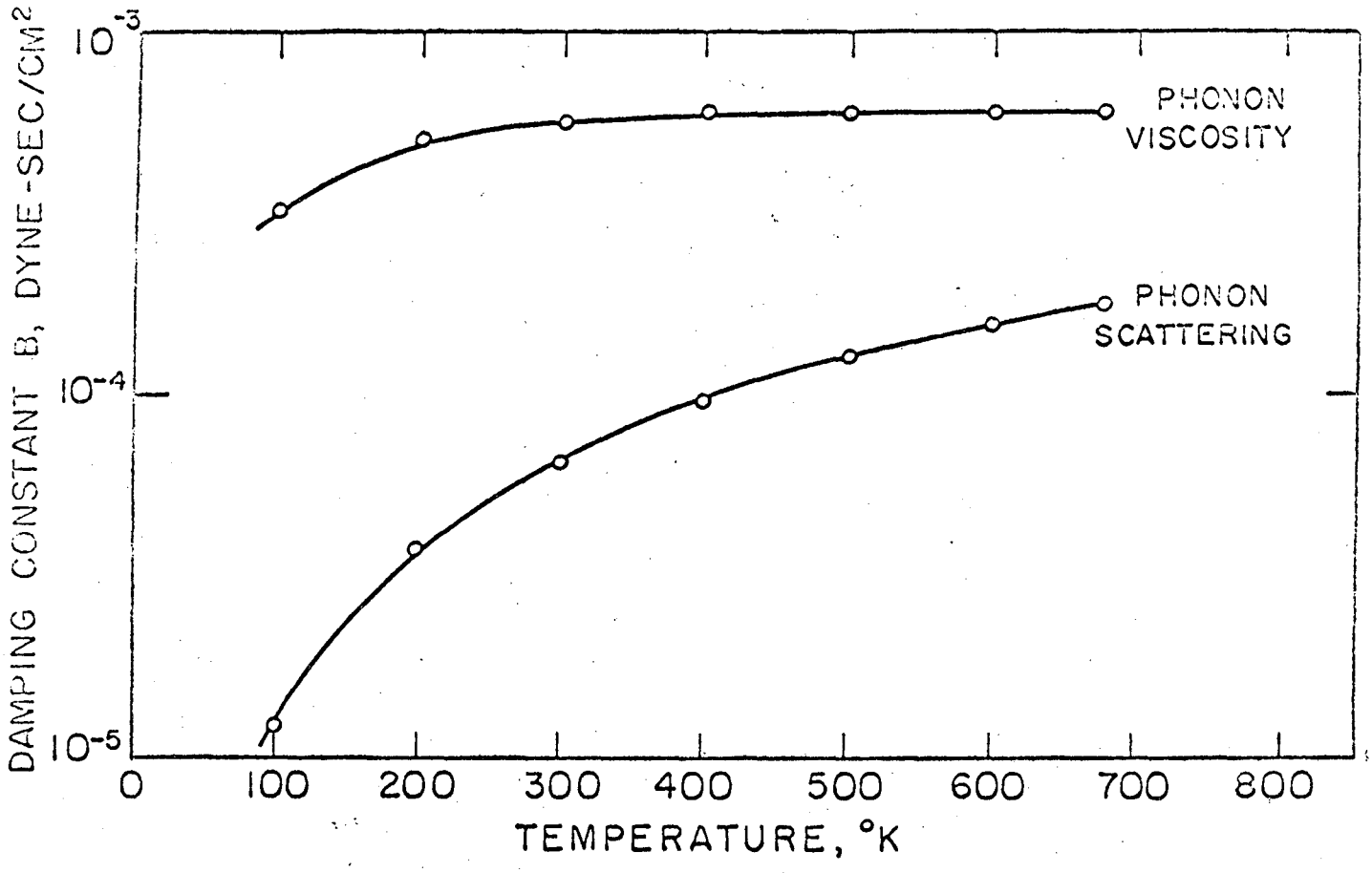

FIG. 4 THEORETICAL DAMPING CONSTANTS FOR PHONON SCATTERING AND PHONON VISCOSITY VERSUS TEMPERATURE.

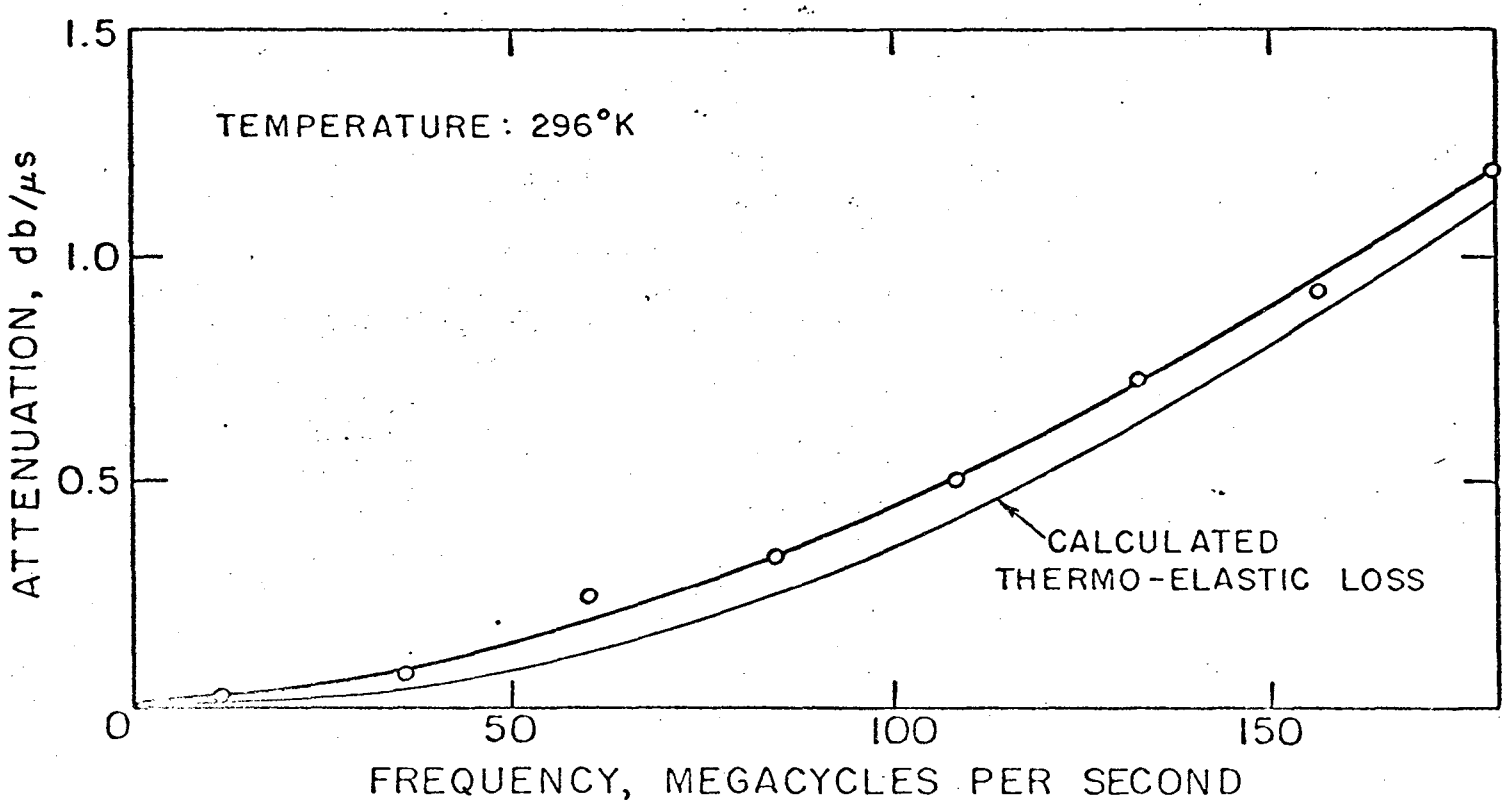

FIG. 5 ATTENUATION FOR THE PROPAGATION OF A LONGITUDINAL WAVE ALONG THE C-AXIS OF A ZINC SINGLE CRYSTAL.[24]

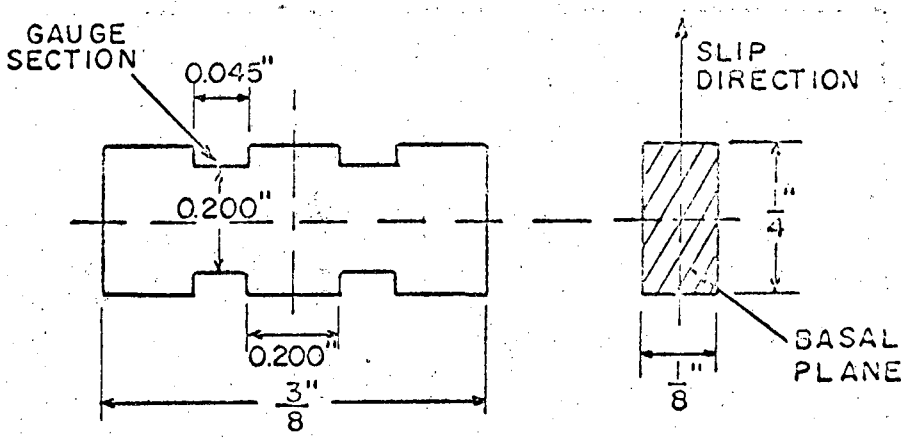

FIG. 2a. SPECIMEN GEOMETRY.

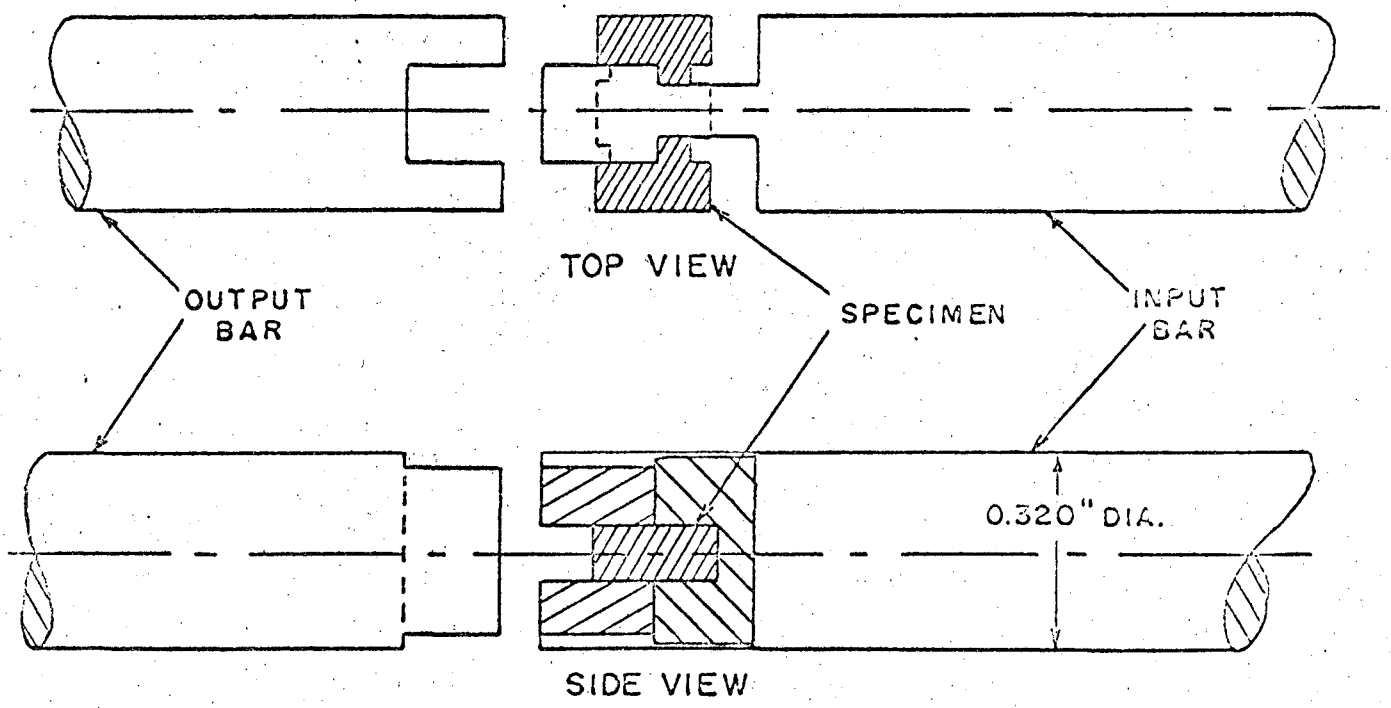

FIG. 2b. SHEAR BARS USED FOR DYNAMIC TESTING.

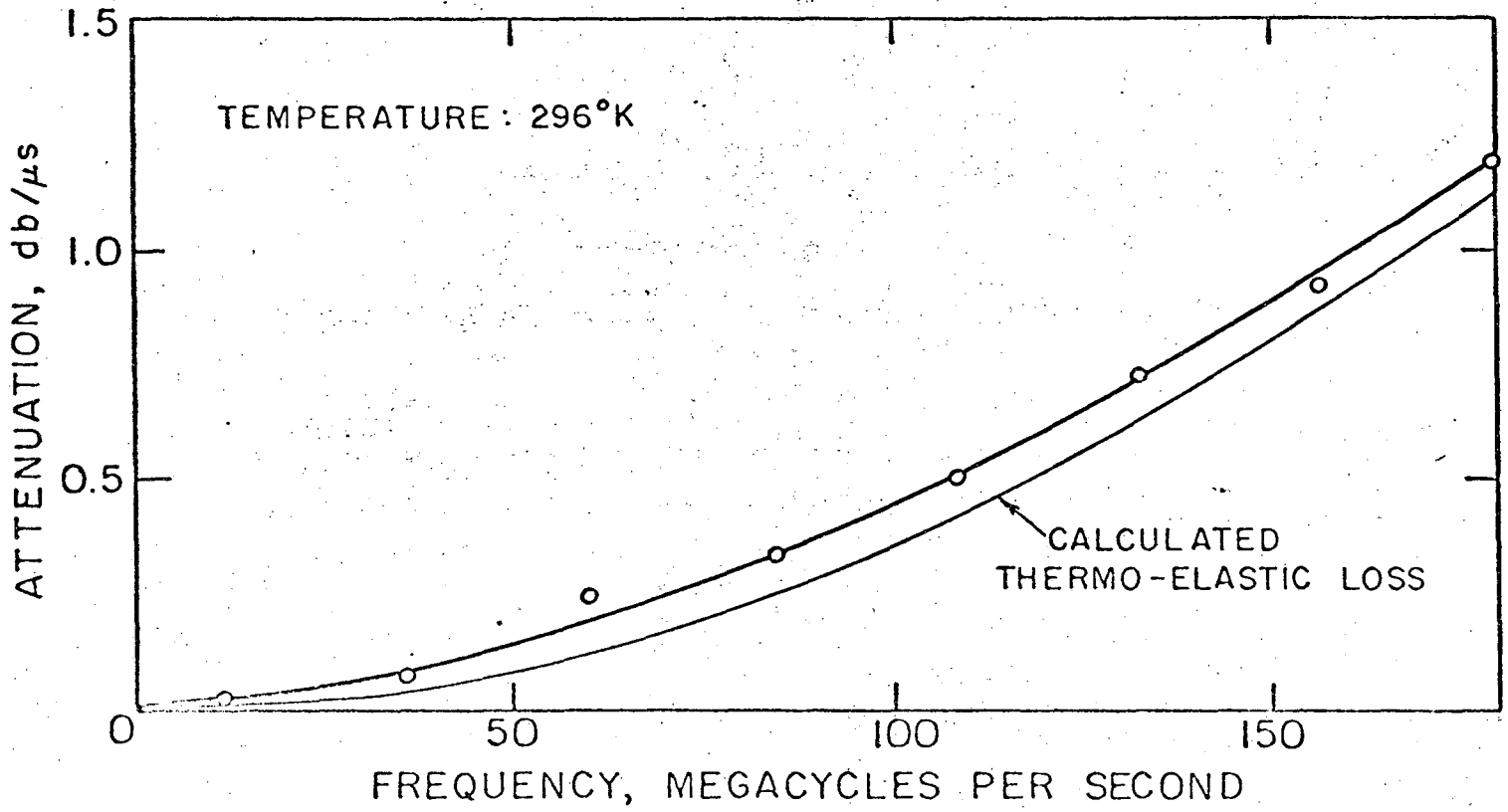

FIG. 5 ATTENUATION FOR THE PROPAGATION OF A LONGITUDINAL WAVE ALONG THE C-AXIS OF A ZINC SINGLE CRYSTAL.[24]